

The absorption of wave energy by a three-dimensional submerged duct

By J. R. THOMAS

School of Mathematics, University of Bristol, University Walk, Bristol BS8 1TW

(Received 20 May 1980)

It has been shown (Evans 1976) that the power absorbed by a general, axisymmetric body depends solely upon the added-mass and damping coefficients. These coefficients are fundamental properties of the body, representing the component of the force on the body proportional to the acceleration and velocity of the body respectively in the radiation problem, where the body is forced to oscillate in the absence of incoming waves.

In the present paper these coefficients are determined by solution of the radiation problem, for a mouth-upward cylindrical duct situated on the sea bed and fitted with a piston undergoing forced oscillations. The added-mass and damping coefficients are then used to study the power absorption properties of the duct when the power take-off is modelled by a linear-spring-dashpot system attached to the piston. Curves of the added mass, damping coefficients and absorption length (a measure of the power absorbed) as functions of wavenumber are presented, for different duct diameters and different depths of submergence.

1. Introduction

One type of wave-energy absorber under current consideration is the submerged device situated on the sea bed. Although moving away from the sea surface towards the sea bed will, in general, tend to narrow the absorption length† *vs.* wavenumber bandwidth of the device, it has the advantage of shielding the absorber, to some extent, from local storms which could cause damage to a surface device.

Mouth-upward-facing ducts in two dimensions have been studied by Lighthill (1979) using complex analysis to obtain the various important hydrodynamic coefficients. Later work by Simon (1981) extends this to three dimensions, where use is made of reciprocal relations which exist between the scattering and radiation problems in the linear theory, together with an approximate variational technique.

In this paper, we shall consider the three-dimensional case of an upward-facing duct of circular cross-section, fitted with a piston, at sea-bed level for mathematical simplicity, which is attached to a spring-dashpot system as a means of extracting energy. Simon uses a similar model, although he treats the infinite depth case where the power take-off system is now modelled by an energy extraction coefficient (equivalent to a dashpot) applied in the depths of the duct.

Evans (1976) has shown that the absorption length may be determined from

† Absorption length = the ratio of energy absorbed by the device to the energy per unit frontage of incident wave.

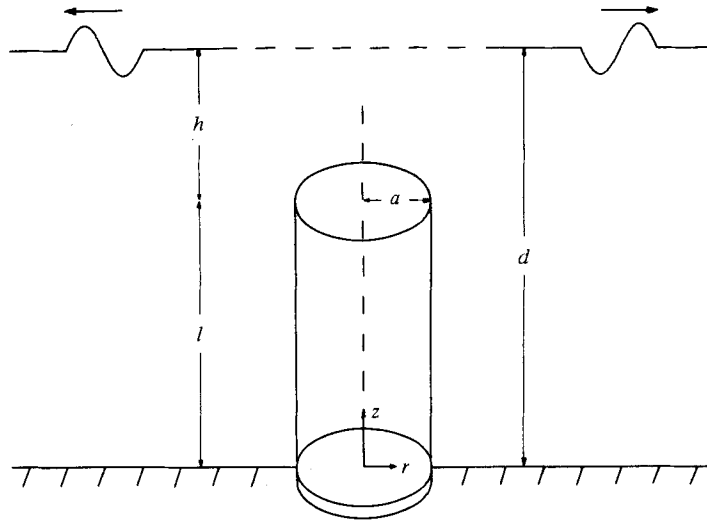


FIGURE 1. Mouth-upward duct of radius a , length l , in water of depth d .

knowledge of fundamental properties of the absorbing body: the added-mass and damping coefficients. Waves incident upon the device will be diffracted, scattering in all directions, and will also set the piston in motion, generating further waves. As explained fully in Newman (1977) the velocity potential can thus be decomposed into scattering potential, where the piston is held fixed in the presence of incoming waves, and a radiation potential, where the piston is forced to oscillate with unit amplitude in the absence of incoming waves. The added-mass and damping coefficients may be obtained by evaluating the hydrodynamic force on the piston in the radiation problem.

Hence, to study the absorption length we need only consider the problem of forced oscillations of the piston. The method of solution relies on finite depth and is due to Garrett, who considered the problems of bottomless harbours (1970) and the wave forces on a circular dock (1971).

Added-mass and damping curves as functions of wavenumber are given in §6. For narrow tubes the added-mass coefficient remains fairly constant over the range considered, being in general slightly larger than the mass of water in the tube. As the tube length increases, it is shown that the absorption-length bandwidth decreases at first before reaching a minimum and increases again as the mouth of the duct approaches the surface. It appears that the main advantage of the tube is that it reduces the piston motion as the tube length increases. A comparison of these coefficients is made with those obtained by Simon (1981) in infinite depth.

The limiting case of an oscillating disk on the sea bed is considered in §5. This is easily solved and provides a useful check on the computation necessary in the above case.

In appendix B the absorption length and amplitude ratio in finite depth are derived for a general axisymmetric heaving body. In the limiting case of infinite depth the expressions agree with those obtained by Evans (1976) and, as in the infinite depth case, the maximum absorption length obtainable by an axisymmetric heaving body is $\lambda/2\pi$, where λ is the wavelength of the incoming waves which is now dependent on the water depth.

2. Formulation

The radiation problem

A submerged vertical tube of length l and circular cross-section of radius a stands on the sea bed in water of depth d ($d > l$). The tube is fitted with a piston, which is forced to oscillate with frequency ω and unit amplitude. We wish to find the hydrodynamic force on the piston and hence the added-mass and damping coefficients of the device.

Cylindrical polar co-ordinates (r, θ, z) are used with z positive upwards and the origin at the mean position of the centre of the piston (figure 1).

Assuming small displacements and irrotational flow, the fluid motion is governed by classical linearized water-wave theory. There is no θ dependence in the problem by symmetry, so we may introduce a velocity potential,

$$\Phi(r, z, t) = \text{Re}\{\phi(r, z) e^{-i\omega t}\}, \quad (2.1)$$

where, following the usual convention, the time co-ordinate is suppressed. The potential ϕ must satisfy

$$\nabla^2 \phi = \frac{\partial^2 \phi}{\partial r^2} + \frac{1}{r} \frac{\partial \phi}{\partial r} + \frac{\partial^2 \phi}{\partial z^2} = 0 \quad \text{in the fluid,} \quad (2.2)$$

with the linearized boundary conditions

$$K\phi - \frac{\partial \phi}{\partial z} = 0 \quad \text{on the free surface} \quad (z = d), \quad (2.3)$$

where $K = \omega^2/g$,

$$\frac{\partial \phi}{\partial z} = 1 \quad \text{on the piston} \quad (z = 0, \quad r < a), \quad (2.4)$$

$$\frac{\partial \phi}{\partial z} = 0 \quad \text{on the sea bed} \quad (z = 0, \quad r > a), \quad (2.5)$$

$$\frac{\partial \phi}{\partial r} = 0 \quad \text{on the tube} \quad (r = a, \quad 0 \leq z \leq l). \quad (2.6)$$

We also require ϕ to satisfy the appropriate radiation condition,

$$\phi \sim \frac{\mathcal{A} e^{ikr} \cosh kz}{(kr)^{\frac{1}{2}} \cosh kd} \quad \text{as } r \rightarrow \infty, \quad (2.7)$$

where \mathcal{A} is some constant.

We may solve Laplace's equation in the inner ($r \leq a$) and outer ($r \geq a$) regions, giving

$$\phi = \sum_{n=0}^{\infty} B_n K_0(\alpha_n r) Z_n(z) \quad (r \geq a), \quad (2.8)$$

$$\phi = \sum_{n=0}^{\infty} A_n I_0(\alpha_n r) Z_n(z) + [(z-d) + g/\omega^2] \quad (r \leq a), \quad (2.9)$$

where A_n, B_n are unknown constants and, in the notation of Miles & Gilbert (1968),

$$Z_0(z) = N_0^{-\frac{1}{2}} \cosh kz, \quad \text{where } N_0 = \frac{1}{2}[1 + (2kd)^{-1} \sinh 2kd], \quad (2.10)$$

$$Z_n(z) = N_n^{-\frac{1}{2}} \cos \alpha_n z, \quad \text{where } N_n = \frac{1}{2}[1 + (2\alpha_n d)^{-1} \sin 2\alpha_n d], \quad (2.11)$$

for $n \geq 1$.

Here k is the wavenumber related to ω through the dispersion relation

$$\omega^2 = gk \tanh kd \quad (\text{also given by } \alpha_0 = -ik), \tag{2.12}$$

and α_n are the positive real roots of

$$g\alpha \tan \alpha d = -\omega^2, \tag{2.13}$$

with $\alpha_n < \alpha_{n+1}$ ($n \geq 1$).

The $Z_n(z)$ ($n \geq 0$) form a complete orthogonal set in $[0, d]$ with mean-square values of 1.

Note that

$$K_0(-ikr) = \frac{1}{2}\pi i H_0(kr), \tag{2.14}$$

$$I_0(-ikr) = J_0(kr), \tag{2.15}$$

where J_0 is an ordinary Bessel function, I_0 and K_0 are modified Bessel functions and H_0 is the zero-order Hankel function of the first kind (the usual superscript may be omitted without ambiguity as a result of the radiation condition).

As in Black, Mei & Bray (1971), we have included a particular solution in the inner region, which is harmonic and satisfies conditions (2.3) and (2.4).

Following Miles & Gilbert (1968) we now construct ϕ in the inner and outer regions in terms of $\partial\phi/\partial r$ at the cylindrical interface $r = a$, $l \leq z \leq d$.

Suppose

$$\frac{\partial\phi}{\partial r} = f(z) \quad \text{at } r = a, \quad l \leq z \leq d, \tag{2.16}$$

we have also

$$\frac{\partial\phi}{\partial r} = 0 \quad \text{at } r = a, \quad 0 \leq z \leq l. \tag{2.17}$$

Hence we may expand $\partial\phi/\partial r$ over $0 \leq z \leq d$ as

$$\left. \frac{\partial\phi}{\partial r} \right|_{r=a} = f(z) = \sum_{n=0}^{\infty} \mathcal{F}_n Z_n(z), \tag{2.18}$$

where

$$\mathcal{F}_n = \frac{1}{d} \int_l^d f(z) Z_n(z) dz. \tag{2.19}$$

The representations of ϕ in the inner and outer regions now become

$$\phi = \sum_{n=0}^{\infty} \frac{\mathcal{F}_n K_0(\alpha_n r)}{\alpha_n K'_0(\alpha_n a)} Z_n(z) \quad (r \geq a), \tag{2.20}$$

$$\phi = \sum_{n=0}^{\infty} \frac{\mathcal{F}_n I_0(\alpha_n r)}{\alpha_n I'_0(\alpha_n a)} Z_n(z) + \left[(z-d) + \frac{g}{\omega^2} \right] \quad (r \leq a). \tag{2.21}$$

The pressure, and hence ϕ , is continuous at $r = a$, $l \leq z \leq d$, so matching the solution in the inner and outer regions gives

$$\sum_{n=0}^{\infty} \mathcal{F}_n \left\{ \frac{K_0(\alpha_n a)}{\alpha_n K'_0(\alpha_n a)} - \frac{I_0(\alpha_n a)}{\alpha_n I'_0(\alpha_n a)} \right\} = (z-d) + \frac{g}{\omega^2} \tag{2.22}$$

valid for $l \leq z \leq d$.

This may be simplified using the formula (Abramowitz & Stegun 1970)

$$-I_0(\alpha_n a) K'_0(\alpha_n a) + I'_0(\alpha_n a) K_0(\alpha_n a) = (\alpha_n a)^{-1} \quad \text{for } n \geq 0. \tag{2.23}$$

Define

$$R_n = -[\alpha_n^2 a^2 I_0'(\alpha_n a) K_0'(\alpha_n a)]^{-1} \quad \text{for } n \geq 0, \quad (2.24)$$

and equation (2.22) then becomes

$$\sum_{n=0}^{\infty} \mathcal{F}_n R_n Z_n(z) = \frac{1}{a} [(d-z) - g/\omega^2], \quad l \leq z \leq d. \quad (2.25)$$

3. Solution

Miles & Gilbert proceeded to set up an integral equation; however we shall adopt the approach of Garrett and construct an infinite system of simultaneous linear equations for the unknown \mathcal{F}_n .

Over $0 \leq z \leq l$ we have, from equation (2.6)

$$\sum_{n=0}^{\infty} \mathcal{F}_n Z_n(z) = 0. \quad (3.1)$$

Multiply (2.25) and (3.1) by $Z_m(z)$, integrate over region of validity, divide by d and add. Thus

$$\sum_{n=0}^{\infty} E_{mn} \mathcal{F}_n = C_m, \quad (3.2)$$

where

$$E_{mn} = (R_n - 1) D_{mn} + \delta_{mn}, \quad (3.3)$$

$$D_{mn} = \frac{1}{d} \int_l^d Z_m(z) Z_n(z) dz \quad (3.4)$$

and

$$C_m = \frac{1}{ad} \int_l^d [(d-z) - g/\omega^2] Z_m(z) dz \quad (3.5)$$

(see appendix A for expressions for D_{mn} , C_m).

The above is a complex matrix equation which can be reduced to two real matrix equations, more easily solved by the computer, by writing

$$\mathcal{F}_n = a_n + ib_n, \quad (3.6)$$

where a_n , b_n are real, and uncoupling the resulting equation (see Ogilvie 1963).

Note that E_{mn} is real except for $n = 0$ (since $R_0 = -[\frac{1}{2}\pi ik^2 a^2 J_0'(ka) H_0'(ka)]^{-1}$). Writing

$$E_{m0} = \gamma_m + i\beta_m \quad (m \geq 0), \quad (3.7)$$

where γ_m , β_m are real (see appendix A for expressions for γ_m , β_m), then from (3.2) we have

$$\sum_{n=1}^{\infty} E_{mn} (a_n + ib_n) + (\gamma_m + i\beta_m) (a_0 + ib_0) = C_m. \quad (3.8)$$

Equate real and imaginary parts to obtain

$$\sum_{n=1}^{\infty} E_{mn} a_n + \gamma_m a_0 = C_m + b_0 \beta_m, \quad (3.9)$$

$$\sum_{n=1}^{\infty} E_{mn} b_n + \gamma_m b_0 = -a_0 \beta_m. \quad (3.10)$$

If ϵ_n, δ_n are the solutions of

$$\gamma_m \epsilon_0 + \sum_{n=1}^{\infty} E_{mn} \epsilon_n = C_m, \quad (3.11)$$

$$\gamma_m \delta_0 + \sum_{n=1}^{\infty} E_{mn} \delta_n = \beta_m, \quad m = 0, 1, 2, \dots, \quad (3.12)$$

then

$$a_n = \epsilon_n + b_0 \delta_n, \quad (3.13)$$

$$b_n = -a_0 \delta_n, \quad n = 0, 1, 2, \dots, \quad (3.14)$$

and, in particular,

$$a_0 = \epsilon_0 + b_0 \delta_0, \quad b_0 = -a_0 \delta_0. \quad (3.15)$$

Thus

$$a_0 = \frac{\epsilon_0}{1 + \delta_0^2}, \quad b_0 = -\frac{\epsilon_0 \delta_0}{1 + \delta_0^2}, \quad (3.16)$$

and

$$\begin{aligned} \mathcal{F}_n &= a_n + ib_n \\ &= \left\{ \epsilon_n - \frac{\epsilon_0 \delta_0 \delta_n}{1 + \delta_n^2} \right\} + i \left\{ -\frac{\epsilon_0 \delta_n}{1 + \delta_n^2} \right\}, \quad n \geq 0. \end{aligned} \quad (3.17)$$

So, upon solving the two real systems of equations (3.11), (3.12) (the method employed is given in §6.3), we can evaluate \mathcal{F}_n ($n \geq 0$) and obtain a full solution for ϕ from equations (2.20), (2.21).

4. Calculation of added-mass and damping coefficients and energy extraction

4.1. Added-mass and damping coefficients

It is shown in Newman (1977) that the complex force in the i th direction due to a sinusoidal motion of frequency ω and unit amplitude in the j th direction may be written in the form

$$f_{ij} = \omega^2 a_{ij} + i\omega b_{ij}, \quad (4.1)$$

where a_{ij}, b_{ij} are the added-mass and damping coefficients respectively, both real and dependent on frequency ω . It is also shown that by integrating the pressure over the body surface, \mathcal{S}_B ,

$$f_{ij} = \rho \int_{\mathcal{S}_B} \frac{\partial \phi_i}{\partial n} \phi_j dS, \quad (4.2)$$

where ϕ_i is the potential corresponding to motion in the i th direction and \mathbf{n} is the unit normal vector on the body surface, directed into the fluid.

In this case the only moveable part of the body is the piston, which is restricted to motion in the z direction; hence only a_{33}, b_{33} are non-zero and

$$f_{33} = \omega^2 a_{33} + i\omega b_{33} \quad (4.3)$$

$$= \rho \int_{\mathcal{S}} \frac{\partial \phi_3}{\partial z} \phi_3 dS, \quad (4.4)$$

where \mathcal{S} is the piston surface. (For convenience, a_{33}, b_{33} will hereafter be denoted by a_3, b_3 .)

Since the motion is of unit amplitude we require

$$\frac{\partial \phi_3}{\partial z} = -i\omega \quad \text{on } \mathcal{S}, \quad (4.5)$$

and thus ϕ_3 is related to the potential ϕ defined in §2 in the following way,

$$\phi_3 = -i\omega\phi \quad (4.6)$$

using (2.4).

Hence

$$\omega^2 a_3 + i\omega b_3 = -\rho\omega^2 \int_{\mathcal{S}} \phi \, dS. \quad (4.7)$$

Using the representation of ϕ in the inner region (2.21),

$$\omega^2 a_3 + i\omega b_3 = -\rho\omega^2 \int_{r=0}^a \int_{\theta=0}^{2\pi} \left[(g/\omega^2 - d) + \sum_{n=0}^{\infty} \frac{\mathcal{F}_n I_0(\alpha_n r)}{\alpha_n I_0'(\alpha_n a)} Z_n(0) \right] r \, dr \, d\theta \quad (4.8)$$

$$= -2\pi\rho\omega^2 \left[(g/\omega^2 - d) \int_0^a r \, dr + \sum_{n=0}^{\infty} \frac{\mathcal{F}_n N_n^{-\frac{1}{2}}}{\alpha_n I_0'(\alpha_n a)} \int_0^a I_0(\alpha_n r) r \, dr \right] \quad (4.9)$$

$$= -2\pi\rho\omega^2 \left[(g/\omega^2 - d) \frac{a^2}{2} + \sum_{n=0}^{\infty} \frac{aN_n^{-\frac{1}{2}} \mathcal{F}_n}{\alpha_n^2} \right]. \quad (4.10)$$

Thus

$$a_3 = 2\pi\rho \left[(d - g/\omega^2) \frac{a^2}{2} + \text{Re} \sum_{n=0}^{\infty} \frac{aN_n^{-\frac{1}{2}} \mathcal{F}_n}{\alpha_n^2} \right], \quad (4.11)$$

$$b_3 = -2\pi\rho\omega \left[\text{Im} \sum_{n=0}^{\infty} \frac{aN_n^{-\frac{1}{2}} \mathcal{F}_n}{\alpha_n^2} \right]. \quad (4.12)$$

4.2. Absorption length and amplitude ratio

The power absorption length is defined by

$$l_d = \frac{\text{power absorbed by body}}{\text{total power in incident wave of unit frontage}},$$

and it can be shown that for the finite depth case (see appendix B)

$$l_d = \frac{4(\omega^2/k) b_3 \bar{d}}{(\bar{k} - a_3 \omega^2)^2 + \omega^2 (b_3 + \bar{d})^2}, \quad (4.13)$$

for a light piston with spring and damper constants \bar{k} , \bar{d} respectively. Now l_d may be rewritten as

$$l_d = \frac{1}{k} \left\{ 1 - \frac{(\bar{k} - a_3 \omega^2)^2 + \omega^2 (\bar{d} - b_3)^2}{(\bar{k} - a_3 \omega^2)^2 + \omega^2 (\bar{d} + b_3)^2} \right\}, \quad (4.14)$$

giving a maximum value of

$$l_{d\max} = \frac{1}{k} = \frac{\lambda}{2\pi}, \quad (4.15)$$

where λ is the wavelength of the incident wave, when

$$\bar{k} = a_3 \omega^2, \quad \bar{d} = b_3. \quad (4.16)$$

The result (4.15) agrees with the infinite depth case (Evans 1976).

Similarly the expression for the ratio of the piston amplitude ξ to the amplitude of the incident wave A , can be shown to be

$$\left| \frac{\xi}{A} \right|^2 = \frac{4\rho c_g b_3}{k [(\bar{k} - a_3 \omega^2)^2 + \omega^2 (b_3 + \bar{d})^2]}, \quad (4.17)$$

which again agrees with the deep water case as $d \rightarrow \infty$, when the group velocity $c_g \rightarrow g/2\omega$.

Before computing values of the added mass and damping we non-dimensionalize by

$$a_3 = M\mu, \quad b_3 = M\omega\lambda, \quad (4.18)$$

where

$$\begin{aligned} M &= \text{mass of water above piston contained in a cylinder of radius } a \\ &= \pi a^2 \rho d, \end{aligned}$$

choosing this particular M instead of the mass of water in the tube so that we are able to consider the limiting case as the length of the tube tends to zero.

If we introduce a non-dimensional wavenumber $\nu = \omega^2 d/g$, then

$$\mu = 1 - \frac{1}{\nu} - 2 \left(\frac{d}{a} \right) \left[\operatorname{Re} \sum_{n=0}^{\infty} \frac{N_n^{-\frac{1}{2}} \mathcal{F}_n}{(\alpha_n d)^2} \right], \quad (4.19)$$

$$\lambda = -2 \left(\frac{d}{a} \right) \left[\operatorname{Im} \sum_{n=0}^{\infty} \frac{N_n^{-\frac{1}{2}} \mathcal{F}_n}{(\alpha_n d)^2} \right]. \quad (4.20)$$

Further, we may 'tune' the system to a frequency ω_0 to give l_d a maximum at this frequency, by assuming we may choose

$$\bar{k} = a_3(\omega_0) \omega_0^2, \quad \bar{d} = b_3(\omega_0). \quad (4.21)$$

Then we have

$$\frac{l_d}{2a} = \frac{1}{2ka} \frac{4\nu(\nu^{\frac{1}{2}}\lambda)(\nu_0^{\frac{1}{2}}\lambda_0)}{[(\mu_0\nu_0 - \mu\nu)^2 + \nu(\nu_0^{\frac{1}{2}}\lambda_0 + \nu^{\frac{1}{2}}\lambda)^2]}, \quad (4.22)$$

$$\left| \frac{\xi}{A} \right|^2 = \frac{\left(\frac{2\lambda}{\pi\nu} \right) \left(\frac{d}{a} \right)^2 (\tanh kd + kd \operatorname{sech}^2 kd)}{[(\mu_0\nu_0 - \mu\nu)^2 + \nu(\nu_0^{\frac{1}{2}}\lambda_0 + \nu^{\frac{1}{2}}\lambda)^2]}, \quad (4.23)$$

where $\nu_0 = \omega_0^2 d/g$, $\mu_0 = \mu(\omega_0)$, $\lambda_0 = \lambda(\omega_0)$.

So, for each value of the non-dimensional wavenumber ν , we solve the two real linear systems of equations given by (3.11), (3.12) to evaluate \mathcal{F}_n ($n \geq 0$) and hence μ and λ . Once the variation of μ and λ with ν is known, and a tuning frequency ω_0 is chosen we can use (4.22), (4.23) to study the absorption length and amplitude ratio variation with ν .

The results obtained are presented and discussed in §6. But first we shall examine the limiting case of an oscillating disk in some detail. It is not a practical absorber but the problem can be easily solved and the behaviour of the added-mass and damping coefficients studied.

5. Limiting disk case

5.1. Statement of problem and solution

An interesting limiting case of the resonant tube is that of an oscillating disk on the sea bed. The approach to the problem is as for the tube, but the fact that we are now matching ϕ at $r = a$ over the whole interval $[0, d]$ produces much simplified results providing a better insight into the behaviour of the added-mass and damping coefficients (the similar curves produced in the disk and tube cases indicate that this behaviour is relevant to the tube problem).

The formulation of the problem is clearly identical with that of the tube case, giving now, instead of (2.25)

$$\sum_{n=0}^{\infty} \mathcal{F}_n R_n Z_n(z) = [(d - g/\omega^2) - z]/a \quad \text{holding for } 0 \leq z \leq d. \quad (5.1)$$

As before, multiply both sides by $(1/d) Z_m(z)$ and integrate to obtain

$$\mathcal{F}_m R_m = \frac{1}{ad} \int_0^d [(d - g/\omega^2) - z] Z_m(z) dz \quad (5.2)$$

$$= C_m \quad \text{with } l = 0. \quad (5.3)$$

Thus

$$\mathcal{F}_0 = \frac{C_0}{R_0}, \quad \text{where } C_0 = -\frac{N_0^{-\frac{1}{2}}}{k^2 ad} \quad (\text{see appendix A}), \quad (5.4)$$

$$\mathcal{F}_m = \frac{C_m}{R_m} \quad (m \geq 1) \quad \text{where } C_m = \frac{N_m^{-\frac{1}{2}}}{\alpha_m^2 ad} \quad (\text{see appendix A}). \quad (5.5)$$

Hence

$$\mathcal{F}_0 = \frac{-N_0^{-\frac{1}{2}}}{k^2 ad} \left[-\frac{1}{2} \pi i k^2 a^2 J_0'(ka) H_0'(ka) \right] \quad (5.6)$$

$$= \frac{N_0^{-\frac{1}{2}} \pi}{2} \left(\frac{a}{d} \right) \left[-J_1(ka) Y_1(ka) + i J_1^2(ka) \right], \quad (5.7)$$

since $H_0(ka) = J_0(ka) + i Y_0(ka)$, and

$$\mathcal{F}_m = \frac{N_m^{-\frac{1}{2}}}{\alpha_m^2 ad} \left[-\alpha_m^2 a^2 I_0'(\alpha_m a) K_0'(\alpha_m a) \right] \quad (5.8)$$

$$= N_m^{-\frac{1}{2}} \left(\frac{a}{d} \right) I_1(\alpha_m a) K_1(\alpha_m a) \quad (m \geq 1). \quad (5.9)$$

5.2. Added-mass and damping coefficients

Using (4.11), (4.12) and the fact that the \mathcal{F}_m are real for $m \geq 1$,

$$b_3 = 2\pi\rho\omega a N_0^{-\frac{1}{2}} \text{Im}(\mathcal{F}_0/k^2), \quad (5.10)$$

$$a_3 = 2\pi\rho \left[(d - g/\omega^2) \frac{a^2}{2} - \text{Re} \left(a \sum_{n=0}^{\infty} \frac{N_n^{-\frac{1}{2}}}{\alpha_n^2} \mathcal{F}_n \right) \right], \quad (5.11)$$

giving

$$b_3 = \frac{\pi^2 a^2 \rho \omega}{k^2 d} N_0^{-1} J_1^2(ka), \quad (5.12)$$

$$a_3 = \pi a^2 \rho \left[(d - g/\omega^2) - \frac{N_0^{-1} \pi}{k^2 d} J_1(ka) Y_1(ka) - \frac{2}{d} \sum_{n=1}^{\infty} \frac{N_n^{-1} I_1(\alpha_n a) K_1(\alpha_n a)}{\alpha_n^2} \right]. \quad (5.13)$$

I am indebted to a referee for pointing out that this problem of an oscillating disk may also be solved using a Hankel transformation. This method yields an expression for the damping coefficient identical to (5.12) and the following expression for the added-mass coefficient,

$$a_3 = -2\pi\rho a^2 \int_0^{\infty} \frac{J_1^2(\xi a) (\xi \cosh \xi d - K \sinh \xi d)}{\xi^2 (K \cosh \xi d - \xi \sinh \xi d)} d\xi, \quad (5.14)$$

where the integral is to be interpreted in the sense of the Cauchy principal value. By a suitable choice of contour the integral may be evaluated, giving an expression for the added-mass coefficient identical to (5.13).

We may now non-dimensionalize the result in exactly the same way as in the duct case and compute the absorption width and amplitude ratio variation with wave-number for the disk.

One point to note is that for frequencies where ka is equal to a zero of J_1 we have $b_3 = 0$ and, since (see appendix B) the damping coefficient is proportional to the far-field amplitude, we may conclude that, for an infinite set of frequencies, forced oscillation of the piston produces no outward-propagating waves. This is in accordance with the results of Black, Mei & Bray (1971) where they considered water-wave radiation by rigid oscillating bodies. However, the first zero of $J_1(ka)$ occurs at $ka = 3.83171$, i.e.

$$\frac{2\pi d}{\lambda} \simeq 4 \left(\frac{d}{a} \right) \quad \text{or} \quad \frac{\lambda}{d} \simeq \frac{2\pi}{4} \left(\frac{a}{d} \right).$$

So, assuming the water depth is 40–50 m, then, even when the diameter of the disk is equal to the water depth, the first zero will occur at a wavelength of the order of 30–40 m, which is outside the region of interest for wave-energy devices since the important energy source lies in waves of wavelengths between 100 and 200 m.

5.3. Behaviour of coefficients as $\nu \rightarrow 0$, $\nu \rightarrow \infty$

After non-dimensionalization,

$$\lambda = \frac{N_0^{-1} \pi J_1^2(ka)}{(kd)^2}, \quad (5.15)$$

$$\mu = 1 - \frac{1}{\nu} - \frac{N_0^{-1} \pi}{(kd)^2} J_1(ka) Y_1(ka) - 2 \sum_{n=1}^{\infty} \frac{N_n^{-1} I_1(\alpha_n a) K_1(\alpha_n a)}{(\alpha_n d)^2}, \quad (5.16)$$

where $\nu = \omega^2 d/g$.

We shall now consider the behaviour of these coefficients as $\nu \rightarrow 0$. First we shall remind ourselves of the equations satisfied by ν and α_n ($n \geq 1$),

$$\nu = kd \tanh kd, \quad \alpha_n d \tan \alpha_n d + \nu = 0, \quad (5.17), (5.18)$$

and, thus, as $\nu \rightarrow 0$ we have $\nu \rightarrow (kd)^2$ and $\alpha_n \rightarrow n\pi$.

Using the limiting forms of J_1, Y_1 for small arguments (Abramowitz & Stegun 1970), we have the following behaviour of μ and λ as $\nu \rightarrow 0$,

$$\lambda \rightarrow \pi/4(a/d)^2, \quad (5.19)$$

$$\mu \rightarrow 1 - \frac{4}{\pi^2} \sum_{n=1}^{\infty} I_1(n\pi a/d) K_1(n\pi a/d)/n^2. \quad (5.20)$$

Both λ and μ tend to finite values as $\nu \rightarrow 0$, the series appearing in μ converging fairly rapidly since $I_1(z) K_1(z) \sim \frac{1}{2}z^{-1}$ as $z \rightarrow \infty$. As usual, the absorption length will tend to zero as $\nu \rightarrow 0$ but the amplitude ratio will tend to a finite value. We have, as $\nu \rightarrow 0$, from (4.23) and (5.20) above,

$$\left| \frac{\xi}{A} \right| \rightarrow \frac{1}{(\mu_0 \nu_0)}. \quad (5.21)$$

Now as $\nu \rightarrow \infty$,

$$\nu \sim kd \quad \text{and} \quad \alpha_n d \sim n\pi/2, \quad n = 1, 2, \dots$$

Thus, we have

$$\mu \rightarrow 1 - \frac{16}{\pi^2} \sum_{n=1}^{\infty} I_1\left(\frac{n\pi a}{2d}\right) K_1\left(\frac{n\pi a}{2d}\right) / n^2. \quad (5.22)$$

Again μ incorporates a quickly converging series and tends to a finite value.

5.4. Verification of b_3 result for disk

Haskind (1957) and Newman (1962) have shown that the damping coefficient is related to the 'exciting force' i.e. the force on the body when it is held fixed in the presence of incoming waves. In this case evaluation of the exciting force is straightforward as there are no diffracted waves. It can be shown from (B 15) and (B 20) that

$$b_3 = \frac{k}{4\rho g c_g |A|^2} |F|^2, \quad (5.23)$$

where F is the exciting force on the disk, c_g is the group velocity and A is the amplitude of the incoming waves. Now F can be found by integrating the hydrodynamic pressure over the piston surface when the piston is held fixed in incident waves, thus

$$F = -i\omega\rho \int_{\mathcal{S}} \phi_s ds e^{-i\omega t}, \quad (5.24)$$

where $\Phi_s = \text{Re}\{\phi_s e^{-i\omega t}\}$ is the scattering potential. This is just the incident wave potential as there are no diffracted waves. Hence

$$\phi_s = \frac{gA}{\omega} \frac{\cosh kz}{\cosh kd} e^{ikx} \quad (5.25)$$

(taking waves incident from $x = -\infty$ since direction is of no consequence here).

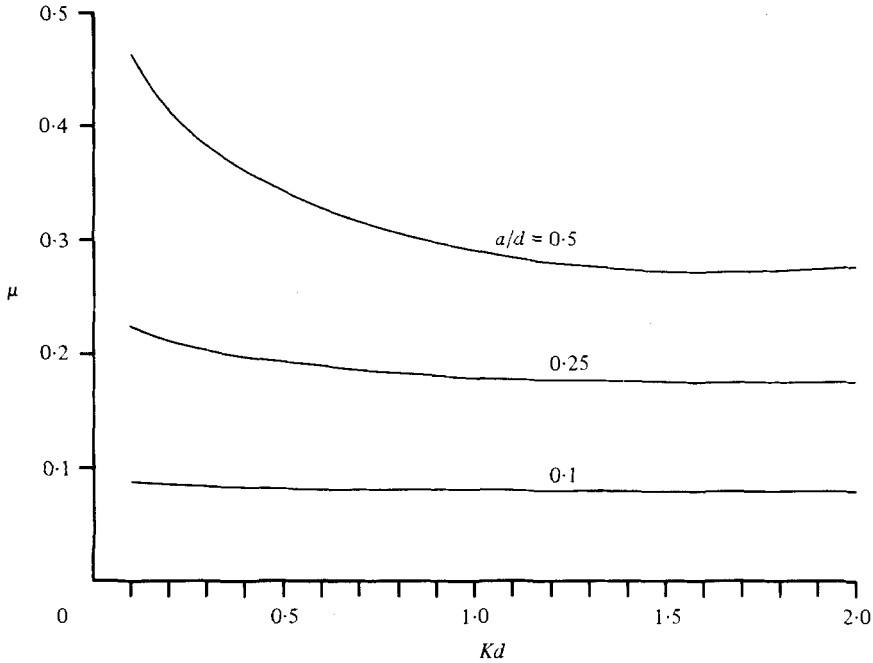


FIGURE 2. Non-dimensional added-mass coefficient μ vs. non-dimensional wavenumber Kd , for the disk, for different values of a/d .

Thus

$$F = -i\omega\rho \int_{r=0}^a \int_{\theta=0}^{2\pi} \phi_s \Big|_{z=0} r dr d\theta e^{-i\omega t} \quad (5.26)$$

$$= \frac{-i\rho g A}{\cosh kd} \int_0^a r dr \int_0^{2\pi} e^{ikr \cos\theta} d\theta e^{-i\omega t}, \quad (5.27)$$

$$= \frac{-i\rho g A}{\cosh kd} \int_0^a 2\pi r J_0(kr) dr e^{-i\omega t} \quad (5.28)$$

$$= \frac{-2\pi i\rho g a A}{k \cosh kd} J_1(ka) e^{-i\omega t}, \quad (5.29)$$

and, substituting for F in (5.23),

$$b_3 = \frac{\pi^2 a \rho g}{kc_\sigma \cosh^2 kd} J_1^2(ka). \quad (5.30)$$

Now, from (2.10), c_σ may be written as

$$c_\sigma = \frac{gkd}{\omega \cosh^2 kd} N_0, \quad (5.31)$$

and, substituting for c_σ in (5.30) using (5.31), it can be seen that the expression for b_3 agrees with that obtained from the radiation problem given by (5.12).

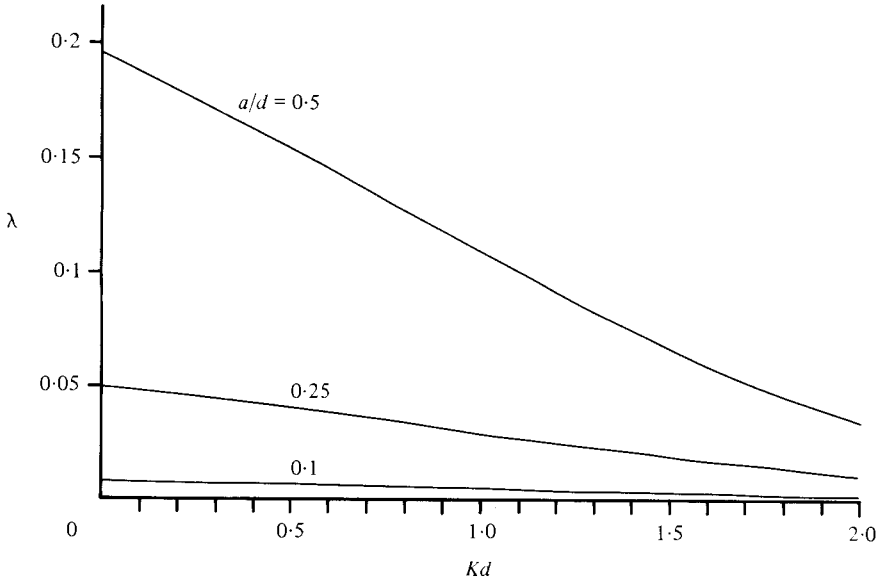


FIGURE 3. Non-dimensional damping coefficient λ vs. non-dimensional wavenumber Kd , for the disk, for different values of a/d .

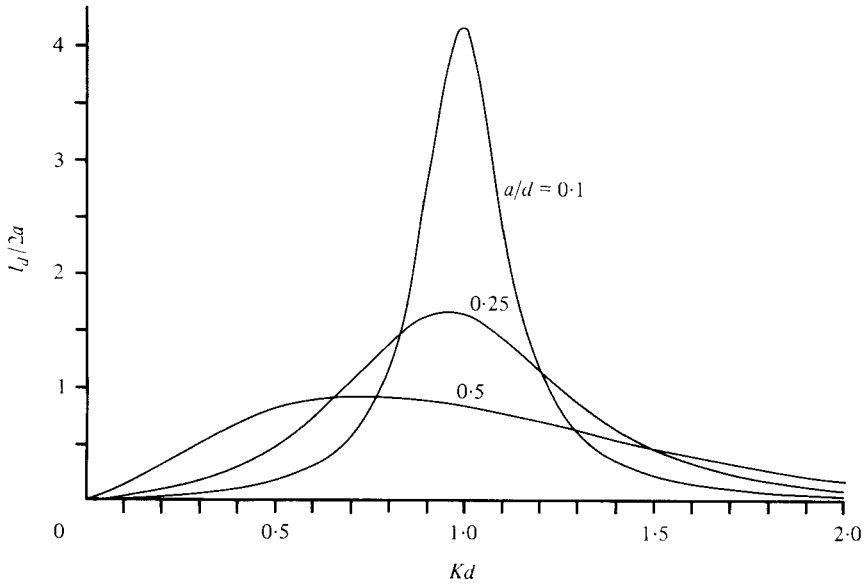


FIGURE 4. Non-dimensional absorption length $l_a/2a$ vs. non-dimensional wavenumber Kd , for the disk, for different values of a/d .

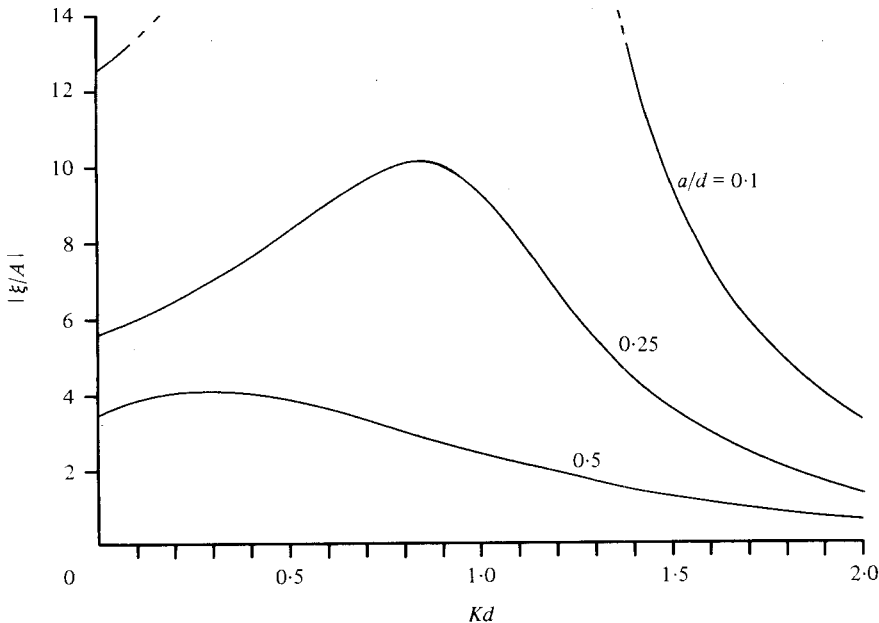


FIGURE 5. Non-dimensional amplitude ratio $|\xi/A|$ vs. non-dimensional wavenumber Kd , for the disk, for different values of a/d .

6. Results and discussion

We shall first examine the results for the disk and then proceed with a study of the duct results.

6.1. The disk on the sea bed

In each case the results for the disk were plotted for values of $a/d = 0.1, 0.25, 0.5$. Figure 2 indicates that, as a/d decreases, so the added-mass variation decreases over the range of ν , and for $a/d = 0.1$ the added mass is fairly constant over the whole range. For $a/d = 0.5$ the curve begins to rise again slightly near $\nu = 2.0$ as the predicted asymptotic value is approached. The damping curves shown in figure 3 illustrate the decrease of the damping coefficient from its asymptotic value at $\nu = 0$ until it reaches its first zero which will occur at a value of $\nu > 2$, when $J_1(ka) = 0$.

We now tune the disk to $\nu_0 = 1.0$ as in §4, and the results are shown in figure 4. For the disk to be a good absorber we require $l_a/2a > 1$ over some appreciable range of values of ν . Physically this means that the disk captures all the power in a wave of crest length greater than the disk diameter. Now $l_{a\max}/2a = (2ka)^{-1}$ so it would seem that, at the tuned wavenumber, we require $kd < \frac{1}{2}(d/a)$. However, as explained in Srokosz (1979), $l_a/2a$ does not attain its maximum value at ν_0 , but to the left of ν_0 . This can be most easily seen when $a/d = 0.5$ in figure 4 and occurs because, although $l_a/2a < (2ka)^{-1}$ for $\nu \neq \nu_0$, $l_a/2a$ is still able to rise above its value at ν_0 and lie below the curve given by $l_{a\max}/2a = (2ka)^{-1}$.

While the curve for $a/d = 0.25$, in particular, seems promising, the amplitude ratio curves shown in figure 5 indicate that the disk oscillations are too large to satisfy the assumption of small amplitude motion required in the linear theory. The magnitude

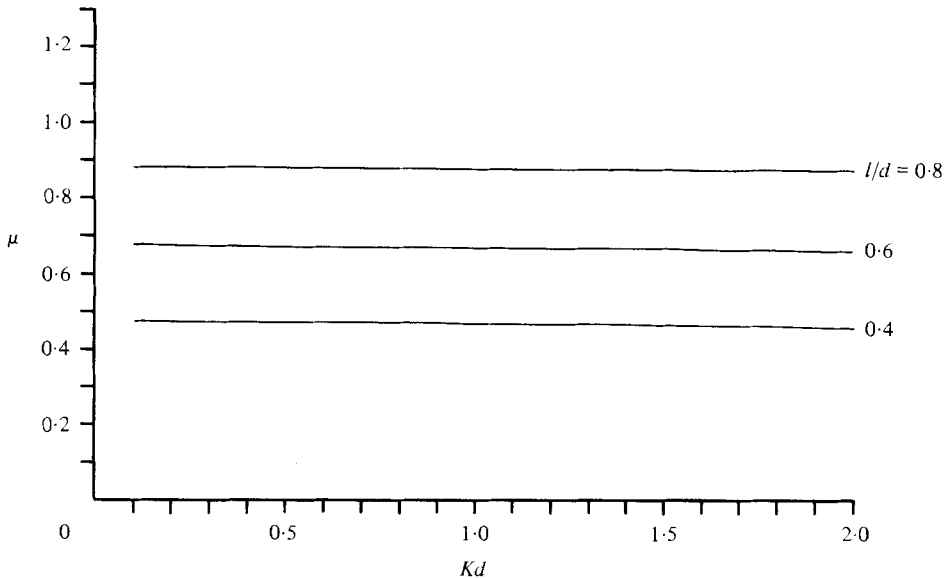


FIGURE 6. Non-dimensional added-mass coefficient μ vs. non-dimensional wave-number Kd , for the duct with $a/d = 0.1$, for different values of l/d .

of these oscillations can be reduced by tuning to smaller wavelengths or increasing the disk diameter, however it is not possible to combine these to make the disk a good absorber while ensuring the motion remains within the bounds of linear theory. So, as expected, the disk is not a good absorber and, indeed, the main purpose of its study was to provide a check for the duct results and to provide analytic expressions for the added-mass and damping coefficients, which in many cases behave similarly to those for the duct.

6.2. The mouth-upward duct

Figure 6 gives the added-mass curves for fixed $a/d = 0.1$ when $l/d = 0.4, 0.6, 0.8$. As for the disk with $a/d = 0.1$, the added mass remains fairly constant over the range of ν , and, in each case, the values of the added mass are slightly larger than the mass of water in the tube. This is since, as a/d gets smaller, the piston is effectively having to move the slug of water in the tube and hence the added mass will approach the mass of water in the tube. (We would expect also an end correction L , as in the case of an open pipe in an infinite fluid with no free surfaces present, where $L = 0.6133a$. However, this value of L will not apply here due to the pressure of the free surface and sea bed.) The damping curves given in figure 7 show some difference from those for the disk case for larger values of l/d , where the damping now rises to a maximum before decreasing to the first zero. (The zeros of the damping were found to occur at the same values that were obtained for the disk: it is not clear why this is so.)

The added-mass and damping curves for fixed $l/d = 0.5$ are shown in figures 8 and 9. Again, the larger variation in the added mass occurs for the wider duct. The damping in each case, although seeming to approach the same value as that for the disk of the same a/d , as $\nu \rightarrow 0$, does not fall off as rapidly as that of the disk as ν increases. Before examining the absorption length and amplitude ratio variation with wave-

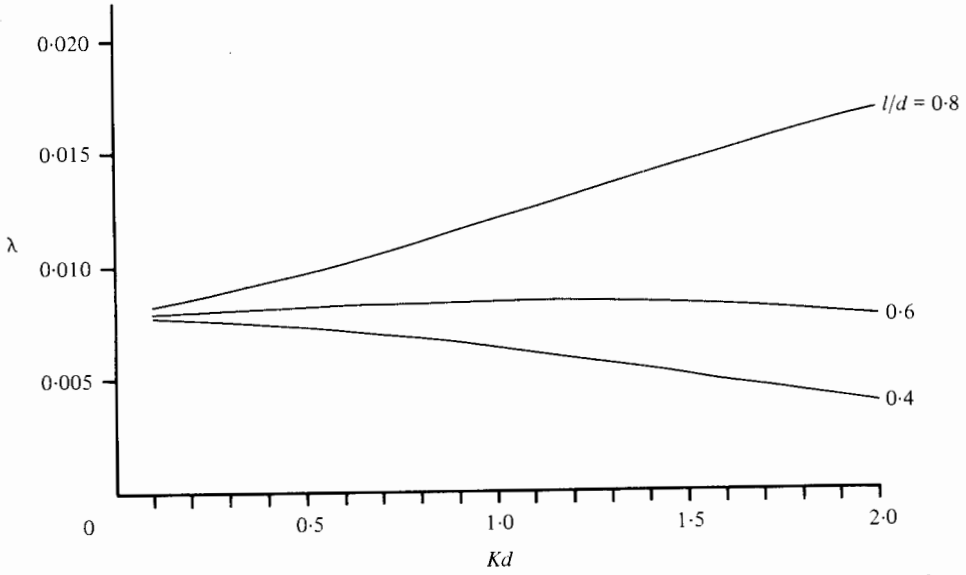


FIGURE 7. Non-dimensional damping coefficient λ vs. non-dimensional wavenumber Kd , for the duct with $a/d = 0.1$, for different values of l/d .

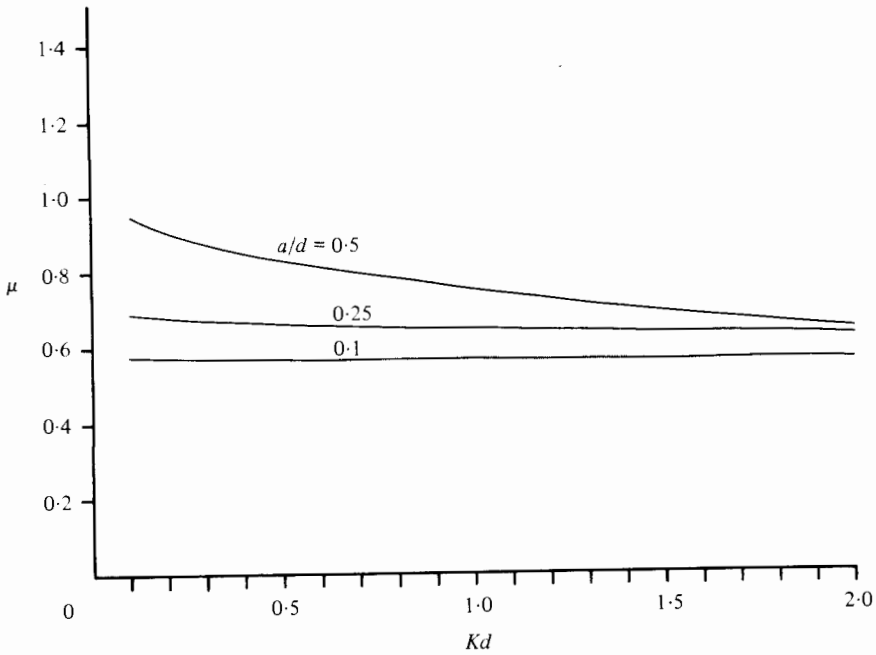


FIGURE 8. Non-dimensional added-mass coefficient μ vs. non-dimensional wavenumber Kd , for the duct with $l/d = 0.5$, for different values of a/d .

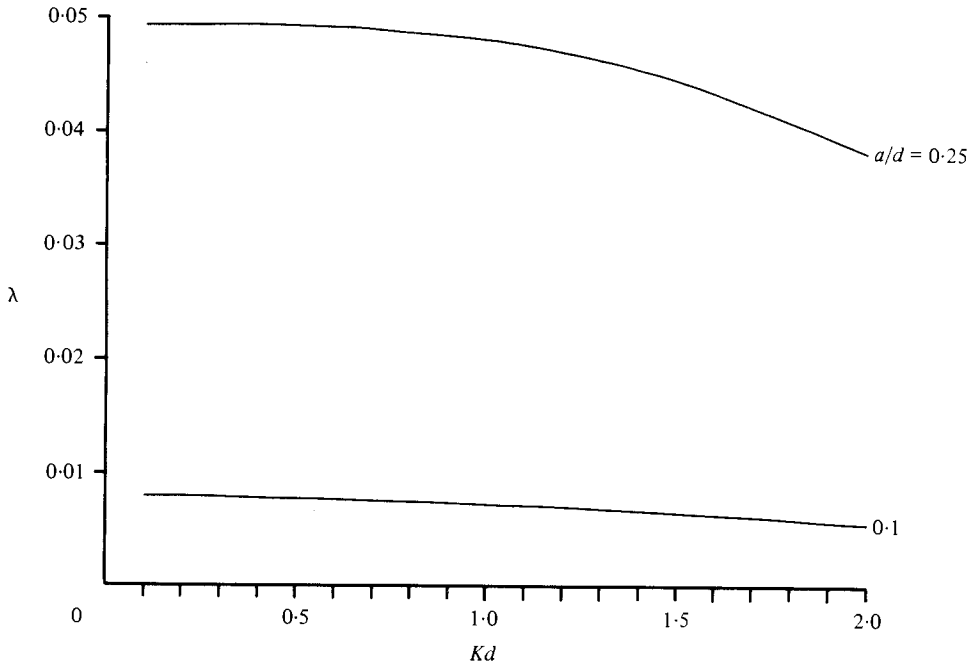


FIGURE 9. Non-dimensional damping coefficient λ vs. non-dimensional wavenumber Kd , for the duct with $l/d = 0.5$, for different values of a/d .

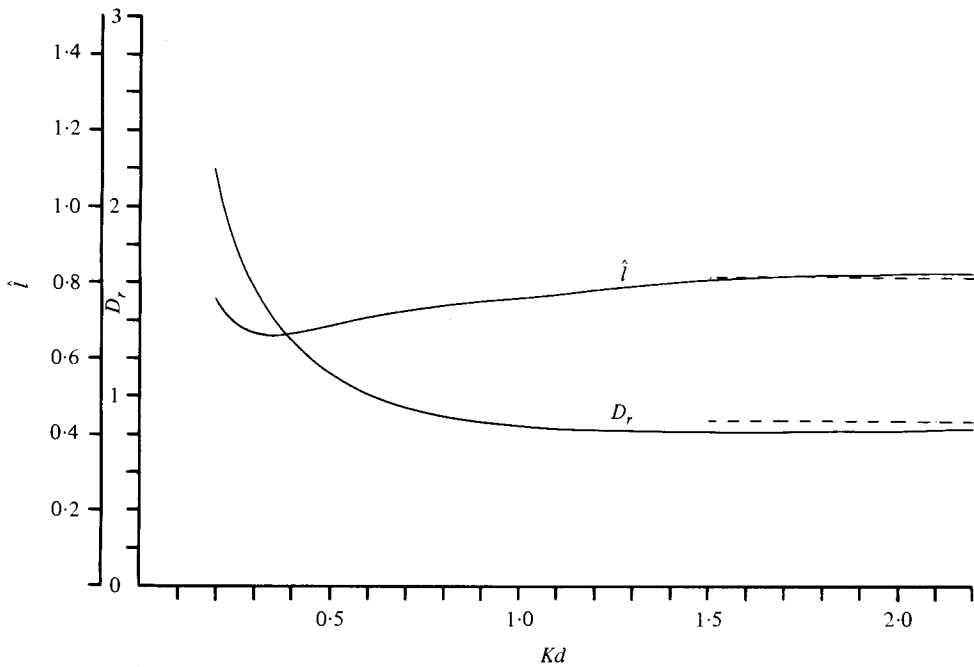


FIGURE 10. Comparison of results for added length \hat{l} , and damping coefficient D_r , vs. non-dimensional wavenumber Kd , with Simon (1981) for $Ka = 0.2$, $Kh = 0.2$. ---, Simon's results in infinite depth; —, results in finite depth.

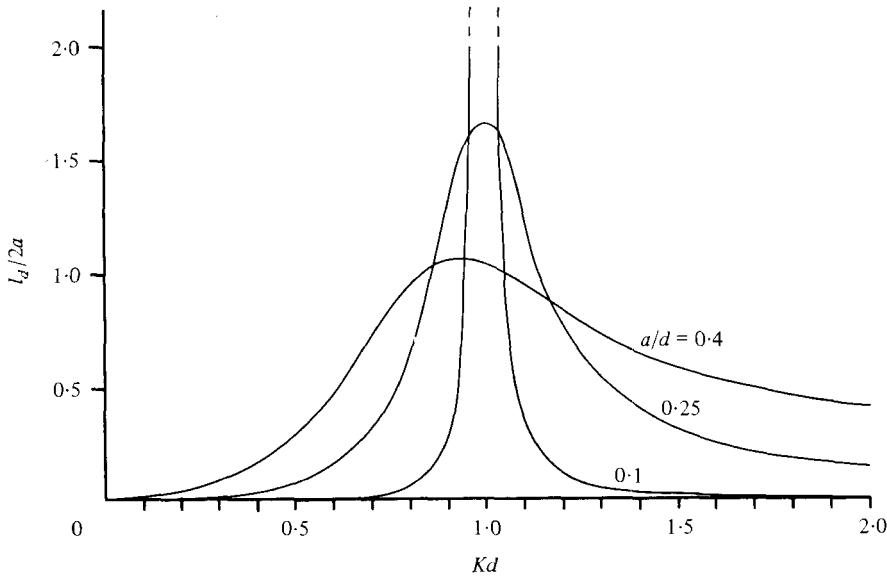


FIGURE 11. Non-dimensional absorption length $l_d/2a$ vs. non-dimensional wavenumber Kd , for the duct with $l/d = 0.8$, $\nu_0 = 1.0$, for different values of a/d .

number we shall study the behaviour of the added-mass and damping coefficients as the depth increases. By fixing $\omega^2 a/g$, $\omega^2 h/g$ and plotting the added mass and damping as functions of $\omega^2 d/g$ we should recover the infinite depth results of Simon (1981) as $\omega^2 d/g \rightarrow \infty$. However, it is first necessary to relate the damping and added mass to the damping coefficient, D_r , and the effective added-length term, \hat{l} , used by Simon. This can be done by examining the respective radiation problems. In the model used here, a piston displacement $\text{Re}[\xi e^{-i\omega t}]$ radiates energy away at a rate $\frac{1}{2}\omega^2 b_3 |\xi|^2$ while, in the radiation problem set up by Simon, a volume flow $\text{Re}[Q e^{i\omega t}]$ in the duct radiates energy away at a rate $\frac{1}{2}\rho\omega K D_r |Q|^2$ (Simon 1981). If we define D_r, \hat{l} in finite depth such that they correspond to D_r, \hat{l} defined in infinite depth by Simon, then after some algebra we find

$$\lambda = \frac{\pi}{2} \left(\frac{a}{\hat{d}}\right) \left(\frac{\omega^2 a}{g}\right) D_r, \quad \mu = \left(\frac{a}{\hat{d}}\right) \left\{\frac{l}{a} + \hat{l}\right\}. \quad (6.1), (6.2)$$

Now, using this definition of D_r, \hat{l} , we should recover the infinite depth values as $\omega^2 d/g \rightarrow \infty$. Figure 10 gives the variation of D_r and \hat{l} with $\omega^2 d/g$, when $\omega^2 a/g = \omega^2 h/g = 0.2$. In all cases, the values seem to be converging to the infinite depth values of Simon (1981). The accuracy of the results decreases as $\omega^2 d/g$ increases and so, for $\omega^2 a/g = 0.2$, it is not possible to be confident about results for $\omega^2 d/g > 2$ say. Note that D_r approaches its infinite depth value from below, although, for $\omega^2 d/g < 0.8$, D_r is greater than its infinite depth value.

Figure 11 shows the absorption length variation for fixed $l/d = 0.8$, with tuned wavenumber once more $\nu_0 = 1.0$. It can be seen that widening the duct diameter will broaden the curve. The same criterion as for the disk applies in determining whether the device is a good absorber; i.e. as a guide we require $kd < \frac{1}{2}(d/a)$ at the tuned wavenumber. So, although the duct could be better tuned, in the case $a/d = 0.1$ say,

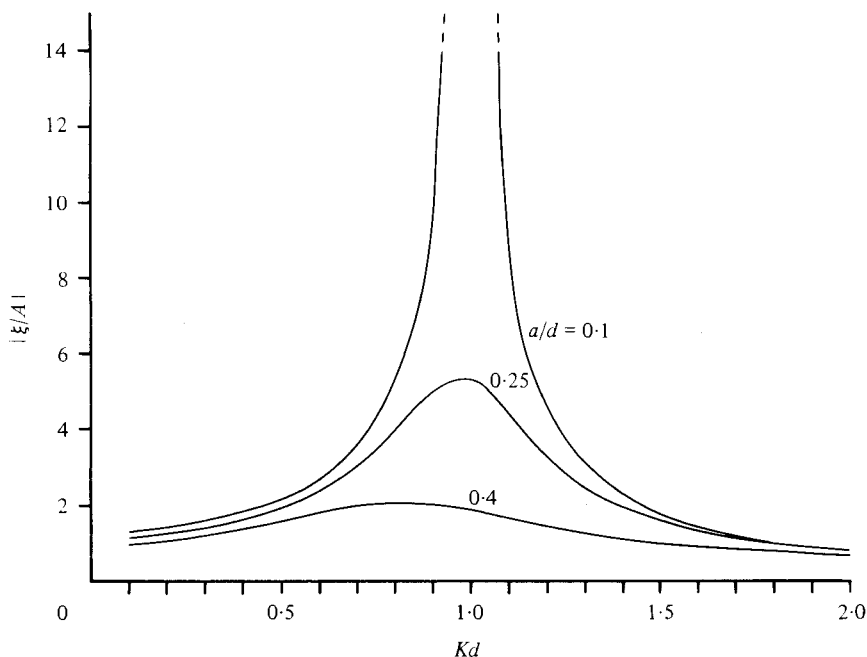


FIGURE 12. Non-dimensional amplitude ratio $|\xi/A|$ vs. non-dimensional wavenumber Kd , for the duct with $l/d = 0.8$, $\nu_0 = 1.0$, for different values of a/d .

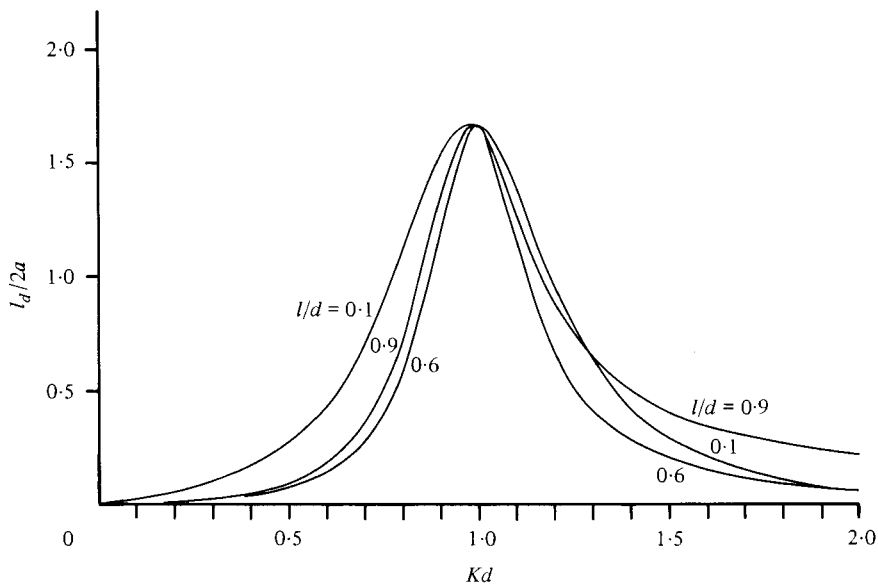


FIGURE 13. Non-dimensional absorption length $l_d/2a$ vs. non-dimensional wavenumber Kd , for the duct with $a/d = 0.25$, $\nu_0 = 1.0$, for different values of l/d .

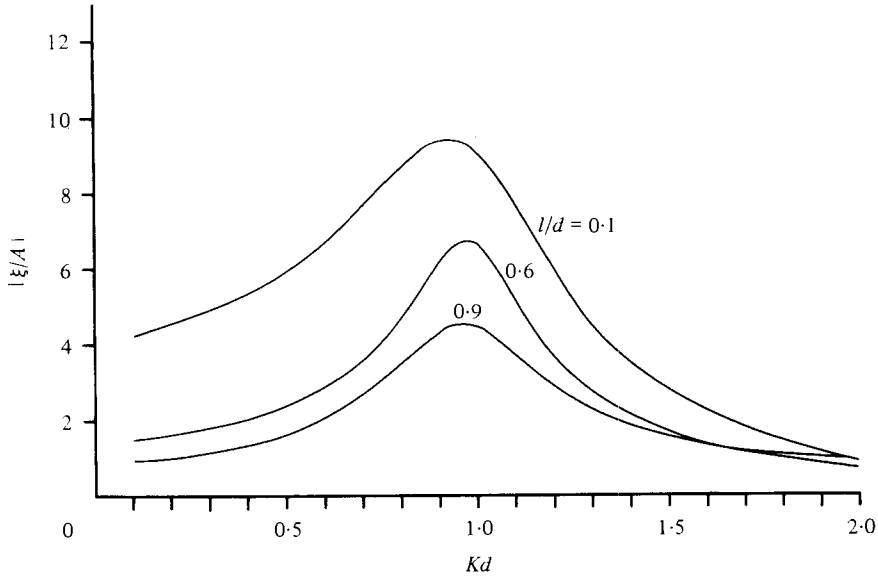


FIGURE 14. Non-dimensional amplitude ratio $|\xi/A|$ vs. non-dimensional wavenumber Kd , for the duct with $a/d = 0.25$, $\nu_0 = 1.0$, for different values of l/d .

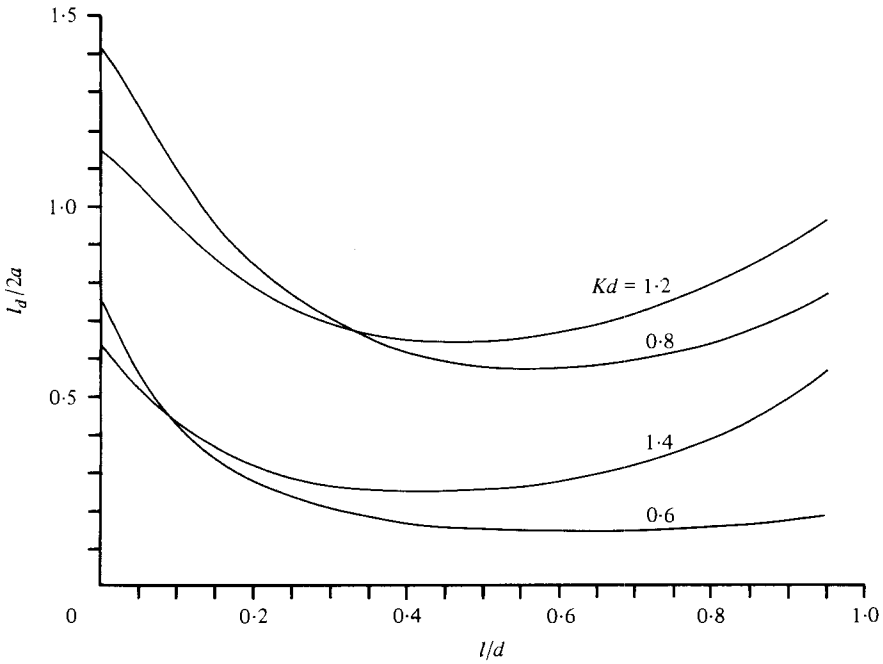


FIGURE 15. Non-dimensional absorption length $l_a/2a$ vs. l/d with $a/d = 0.25$, $\nu_0 = 1.0$, for different values of Kd .

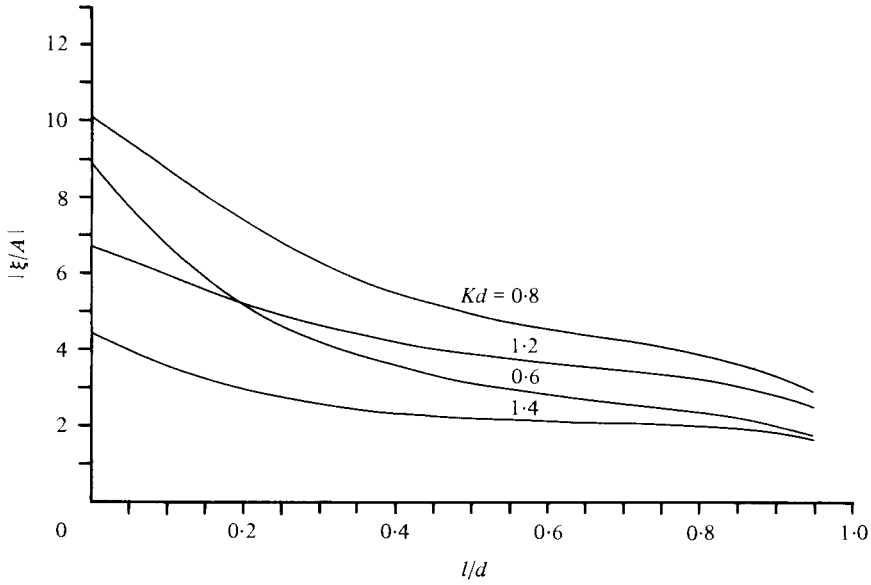


FIGURE 16. Non-dimensional amplitude ratio $|\xi/A|$ vs. l/d with $a/d = 0.25$, $\nu_0 = 1.0$, for different values of Kd .

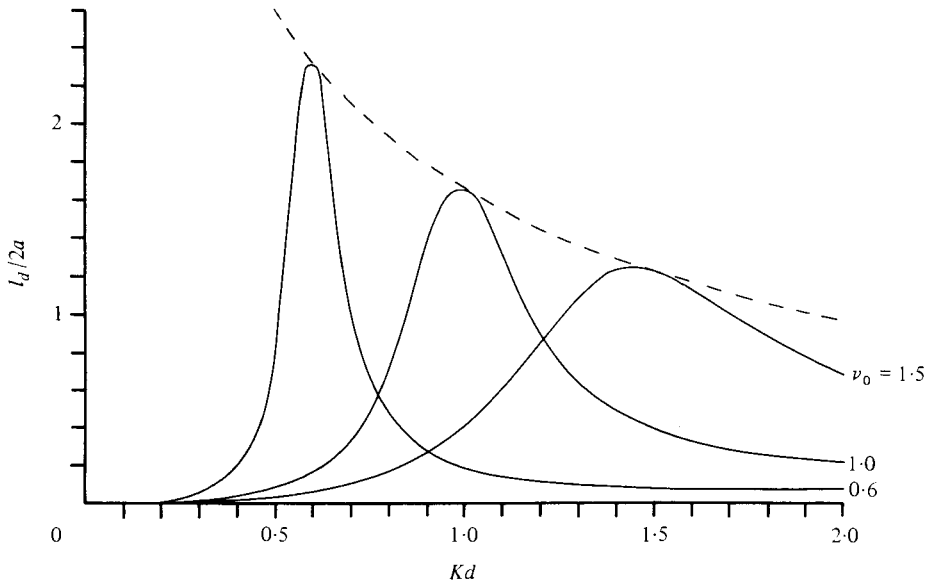


FIGURE 17. Non-dimensional absorption length $l_d/2a$ vs. non-dimensional wavenumber Kd , with $a/d = 0.25$, $l/d = 0.9$ for different values of tuned wavenumber ν_0 . The dashed curve represents the maximum absorption length, $l_{d,max}/2a$.

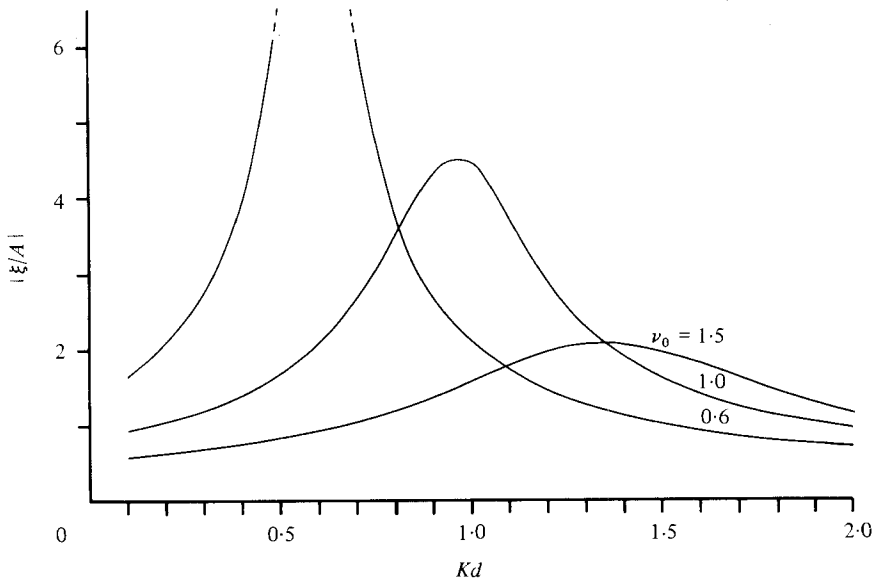


FIGURE 18. Non-dimensional amplitude ratio $|\xi/A|$ vs. non-dimensional wavenumber Kd , with $a/d = 0.25$, $l/d = 0.9$ for different values of tuned wavenumber ν_0 .

figure 12 indicates that the duct diameter should perhaps be too large in order that the assumptions of linear theory be satisfied.

If we now study the absorption length at fixed a/d and vary l/d , the results are not quite so straightforward. As one might expect, figure 13 shows that a wider bandwidth is achieved for $l/d = 0.9$ rather than 0.6, when the duct mouth is closer to the surface. But when $l/d = 0.1$ the bandwidth is wider than in the previous two cases, although the curve does drop off quicker than the curve corresponding to $l/d = 0.9$, as ν increases. On the other hand, the amplitude ratios shown in figure 14 indicate a progressive decrease in $|\xi/A|$ as l/d increases, over practically the whole range, and certainly near the tuned wavenumber. To understand further what is happening here, attention was focused on a fixed value of ν and the variation of absorption length with l/d was studied (figure 15).

Surprisingly, as l/d increases from zero, the bandwidth of the absorption length curve decreases before reaching a minimum and then increases as the duct mouth gets close to the surface. From figure 16 it can be seen that the amplitude ratio falls off rapidly at first before levelling off to some extent until the mouth becomes close to the surface, when it begins to fall again. Apparently, the advantage of the duct is to decrease the amplitude ratio considerably but the tube, in some sense, shields the piston from the incident wave train, although this may be offset by having the duct mouth near the surface.

The effect of tuning to different wavenumbers may be seen in figure 17. The maximum value of $l_d/2a$ is given by the curve $l_{d\max}/2a = (2ka)^{-1}$, shown dotted. Figure 18 shows how the piston oscillations are reduced as ν_0 increases. When $\nu_0 = 0.6$ the absorption length bandwidth is very narrow and the amplitude ratio rises markedly

above the values where linear theory is applicable. But, when $\nu_0 = 1.5$, the amplitude ratio is greatly reduced, as noted in §6.1, linear theory is valid, and the absorption width curve exhibits a broad bandwidth.

6.3. *A note on numerical methods*

We require the solution of two infinite systems of real equations. This was obtained by truncating the systems after N terms and solving the finite system using a standard numerical procedure. Both systems have the same left-hand sides so the matrix of coefficients of ϵ_n , δ_n need only be inverted once numerically. Then, regarding the solutions obtained as functions of N , we require the limit as $N \rightarrow \infty$. By plotting the results against N^{-1} and extrapolating to zero, we may study the convergence of the solutions.

The convergence is slow, being almost linearly dependent on $1/N$ for large N , as Garrett (1970) noted. The equations were solved with $N = 10$, in steps of 10, up to $N = 80$ terms. Unlike Garrett, the solution for $N = 40$ was accurate to within 1% and a linear extrapolation using $N = 40, 50$ compared well with a smooth extrapolation through all the values of N . Using this linear extrapolation, agreement was found to three or four significant figures in general. For smaller values of a/d and certain values of ν , N needs to be larger to maintain the accuracy.

7. Conclusion

In this paper a simplified model of an oscillating water column wave-energy absorber has been used to study the behaviour of the added-mass and damping coefficients and, hence, the absorption length. Expressions for the absorption length and amplitude ratio corresponding to those of Evans (1976) were derived for finite depth, for a general axisymmetric heaving body. The limiting case of an oscillating disk on the sea bed was also analysed, and while this is not a practical device it provided some insight into the behaviour of the added-mass and damping coefficients as well as providing a useful check on the numerical methods used in the duct problem.

The results indicate that, unless a/d is large, the added mass shows relatively little change over the range of ν , while the damping coefficient still retains the zeros found in the disk problem, although the presence of the duct can greatly modify the curves. The added-mass and damping behaviour with increasing depth is presented, showing how these coefficients approach the infinite depth value of Simon (1981).

The variation of absorption length with wavenumber has been illustrated for both fixed a/d and fixed l/d . An unexpected result was that increasing the tube length can actually narrow the bandwidth of the curves. For moderate values of l/d and $2a/d$ the linear theory is not really applicable and, although the amplitude ratio may be reduced, to some extent, by choosing more appropriate tuning wavenumbers, for the device to be a good absorber it is necessary for l/d and $2a/d$ to be quite large, $l/d = 0.9$, $a/d = 0.4$ say.

Thus, such a device situated on the sea bed does not seem practical and better results may be obtained by bringing the device closer to the sea surface. However, it must be pointed out that devices of this type will not be isolated but will appear in arrays where interaction effects can occur which may result in an increase in absorption width.

I would like to thank Dr D.V. Evans for many helpful discussions during the course of this work and the Science Research Council for providing the financial support.

Appendix A

We have

$$D_{mn} = \frac{1}{d} \int_l^d Z_m(z) Z_n(z) dz, \quad (\text{A } 1)$$

giving

$$D_{mn} = (N_n N_m)^{-\frac{1}{2}} [\alpha_n d \sin \alpha_n l \cos \alpha_m l - \alpha_m d \sin \alpha_m l \cos \alpha_n l] / (\alpha_m^2 d^2 - \alpha_n^2 d^2) \quad (\text{A } 2)$$

for $m \neq n, m, n \geq 1$;

$$D_{mm} = \frac{1}{2} \frac{h}{d} N_m^{-1} \left[1 + \frac{\sin \alpha_m h \cos \alpha_m (l+d)}{\alpha_m h} \right] \quad (\text{A } 3)$$

for $m \geq 1$;

$$D_{0n} = D_{n0} = -(N_0 N_n)^{-\frac{1}{2}} [kd \sinh kl \cos \alpha_n l + \alpha_n d \cosh kl \sin \alpha_n l] / (\alpha_n^2 d^2 + k^2 d^2) \quad (\text{A } 4)$$

for $n \geq 1$;

$$D_{00} = \frac{1}{2} \frac{h}{d} N_0^{-1} \left[1 + \frac{\sinh kh \cosh k(l+d)}{kh} \right]. \quad (\text{A } 5)$$

Now

$$C_m = \frac{1}{ad} \int_l^d [(d-z) - g/\omega^2] Z_m(z) dz, \quad (\text{A } 6)$$

giving

$$C_0 = -\frac{N_0^{-\frac{1}{2}}}{ka} \left[\frac{\sinh kh}{kd \sinh kd} + \frac{h}{d} \sinh kl \right], \quad (\text{A } 7)$$

$$C_m = \frac{N_m^{-\frac{1}{2}}}{\alpha_m a} \left[\frac{\sin \alpha_m h}{\alpha_m d \sin \alpha_m d} - \frac{h}{d} \sin \alpha_m l \right] \quad (\text{A } 8)$$

for $m \geq 1$.

We have written, in equation (3.7),

$$E_{m0} = \gamma_m + i\beta_m, \quad (\text{A } 9)$$

where γ_m, β_m are real, for $m \geq 0$; now, from (3.3),

$$E_{m0} = (R_0 - 1) D_{m0} + \delta_{m0}. \quad (\text{A } 10)$$

Thus

$$\gamma_m = \left[\frac{Y_1(ka)}{\frac{1}{2}\pi k^2 a^2 J_1(ka)} (J_1^2(ka) + Y_1^2(ka))^{-1} - 1 \right] D_{m0} + \delta_{m0}, \quad (\text{A } 11)$$

$$\beta_m = \frac{D_{m0}}{\frac{1}{2}\pi k^2 a^2} (J_1^2(ka) + Y_1^2(ka))^{-1}. \quad (\text{A } 12)$$

Note: For the disk case, we have $l = 0$, and so

$$C_0 = -\frac{N_0^{-\frac{1}{2}}}{k^2 ad}, \quad (\text{A } 13)$$

$$C_m = \frac{N_m^{-\frac{1}{2}}}{\alpha_m^2 a d}. \quad (\text{A } 14)$$

Appendix B

Absorption width in finite depth. Consider the full problem of waves incident upon the duct. The equation of motion of the piston is

$$m\ddot{\zeta} + \bar{d}\dot{\zeta} + \bar{k}\zeta = F_T, \quad (\text{B } 1)$$

where \bar{k} , \bar{d} are the spring and damper constants respectively, F_T is the hydrodynamical force on the piston, and

$$\zeta = \text{Re}\{\xi e^{-i\omega t}\} \quad (\text{B } 2)$$

is the displacement of the piston.

Now

$$F_T = F_d + F_r \quad (\text{B } 3)$$

where F_d is the force on the piston when it is held fixed in the presence of incoming waves (the scattering problem), and F_r is the force on the piston when it is oscillating with displacement ζ in the absence of incoming waves (a radiation problem).

And, by definition,

$$F_r = f_{33}\xi e^{-i\omega t} \quad (\text{real part understood}), \quad (\text{B } 4)$$

where f_{33} is defined in equation (4.1), i.e.

$$F_r = (\omega^2 a_3 + i\omega b_3)\xi e^{-i\omega t}. \quad (\text{B } 5)$$

Substituting in equation (B 1) we obtain

$$F_d = \text{Re}\{[(\bar{k} - (m + a_3)\omega^2) - i\omega(\bar{d} + b_3)]\xi e^{-i\omega t}\}. \quad (\text{B } 6)$$

To calculate F_d . The Haskind relations show that the exciting force depends only on the far-field potential of the radiation potential, and is given by

$$F_d = i\omega\rho e^{-i\omega t} \int_{\mathcal{S}_0} \left(\phi_0 \frac{\partial\phi}{\partial n} - \phi \frac{\partial\phi_0}{\partial n} \right) dS, \quad (\text{B } 7)$$

where $\Phi = \text{Re}\{\phi e^{-i\omega t}\}$ is the radiation potential, defined as in § 2, and \mathcal{S}_0 is a control surface, a cylindrical surface, $r = R$ (excluding base and top), with normal directed towards the origin. The incident wave potential is given by $\Phi_0 = \text{Re}\{\phi_0 e^{-i\omega t}\}$, where

$$\phi_0 = \frac{gA}{\omega} \frac{\cosh kz}{\cosh kd} e^{ikx}, \quad (\text{B } 8)$$

representing a wave of amplitude $|A|$, wavenumber k , in water of finite depth d , and this may be written

$$\phi_0 = \frac{gA}{\omega} \frac{\cosh kz}{\cosh kd} \sum_{m=0}^{\infty} \epsilon_m i^m J_m(kr) \cos m\theta \quad (\text{B } 9)$$

$$= \frac{gA}{\omega} \frac{\cosh kz}{\cosh kd} \sum_{m=0}^{\infty} \frac{\epsilon_m i^m}{2} [H_m^{(1)}(kr) + H_m^{(2)}(kr)], \quad (\text{B } 10)$$

where $\epsilon_0 = 1$, $\epsilon_m = 2$ ($m \geq 1$), and $H_m^{(1)}$, $H_m^{(2)}$ are Hankel functions of the first and second kinds respectively.

As $r \rightarrow \infty$, the radiation condition imposed on ϕ gives

$$\phi \sim A_r H_0^{(1)}(kr) \frac{\cosh kz}{\cosh kd}, \quad (\text{B } 11)$$

where A_r is some (complex) constant.

So taking $r = R$ as control surface and letting $R \rightarrow \infty$, the expression for F_d reduces to

$$F_d = -\frac{\pi i \rho g k A A_r e^{-i\omega t}}{\cosh^2 kd} \int_0^d \cosh^2 kz dz \lim_{R \rightarrow \infty} R [H_0^{(1)}(kr) H_1^{(2)}(kr) - H_0^{(2)}(kr) H_1^{(1)}(kr)]. \quad (\text{B } 12)$$

Thus

$$F_d = -\frac{i \rho g k A A_r}{\cosh^2 kd} N_0 d \frac{4i}{k} e^{-i\omega t}, \quad (\text{B } 13)$$

where use has been made of the asymptotic forms of the Hankel functions for large arguments (Abramowitz & Stegun 1970).

Therefore

$$F_d = \frac{4 \rho g d N_0 A A_r}{\cosh^2 kd} e^{-i\omega t}, \quad (\text{B } 14)$$

or

$$F_d = 4 \rho A A_r c_g \frac{\omega}{k} e^{-i\omega t}, \quad (\text{B } 15)$$

where c_g is the group velocity in depth d .

Now, applying Green's theorem to ϕ and $\bar{\phi}$ ($\bar{\phi}$ represents the complex conjugate of ϕ), it can be shown that

$$\frac{2i}{\rho \omega} b_3 = \int_{\mathcal{S}_0} \left(\phi \frac{\partial \bar{\phi}}{\partial n} - \bar{\phi} \frac{\partial \phi}{\partial n} \right) dS, \quad (\text{B } 16)$$

where \mathcal{S}_0 is the control surface previously defined and, as $R \rightarrow \infty$,

$$\phi \sim A_r H_0^{(1)}(kR) \frac{\cosh kz}{\cosh kd}, \quad (\text{B } 17)$$

$$\bar{\phi} \sim A_r H_0^{(2)}(kR) \frac{\cosh kz}{\cosh kd}, \quad (\text{B } 18)$$

and, substituting for ϕ , $\bar{\phi}$, (B 16) reduces to

$$b_3 = \frac{4 \rho \omega d N_0}{\cosh^2 kd} |A_r|^2 \quad (\text{B } 19)$$

$$= \frac{4 \rho}{gk} c_g \omega^2 |A_r|^2. \quad (\text{B } 20)$$

If we use the expression for F_d in (B 15), (B 6) becomes

$$\frac{4 \rho \omega c_g}{k} A A_r = [(\bar{k} - (m + a_3) \omega^2) - i\omega(\bar{d} + b_3)] \xi. \quad (\text{B } 21)$$

The power absorbed by the system is the mean rate at which work is done on the system by the fluid,

$$P = \frac{\omega}{2\pi} \int_0^{2\pi/\omega} \xi F_T dt = \frac{1}{2} \omega^2 \bar{d} |\xi|^2, \quad (\text{B } 22)$$

and the power per unit frontage of the incident wave is

$$\begin{aligned} P_0 &= (\text{wave energy density}) \times (\text{group velocity}) \\ &= \frac{1}{2} \rho g |A|^2 c_g. \end{aligned} \quad (\text{B } 23)$$

Hence the absorption width l_a is given by

$$l_a = \frac{P}{P_0} \quad (\text{B } 24)$$

$$= \frac{\omega^2}{\rho g c_g} \bar{d} \left| \frac{\xi}{A} \right|^2. \quad (\text{B } 25)$$

Substituting for $|\xi/A|$ from (B 21) and using (B 20) to eliminate $|A_r|$, this becomes

$$l_a = \frac{4(\omega^2/k) b_3 \bar{d}}{[(\bar{k} - (m + a_3) \omega^2)^2 + \omega^2(\bar{d} + b_3)^2]}. \quad (\text{B } 26)$$

Note that for deep water we have $\omega^2 = gk$ and the deep water result is obtained (Evans 1976).

REFERENCES

- ABRAMOWITZ, M. & STEGUN, I. A. 1970 *Handbook of Mathematical Functions* 9th edn. Dover Publications.
- BLACK, J. L., MEL, C. C. & BRAY, M. C. G. 1971 Radiation and scattering of water waves by rigid bodies. *J. Fluid Mech.* **46**, 151-164.
- EVANS, D. V. 1976 A theory for wave-power absorption by oscillating bodies. *J. Fluid Mech.* **77**, 1-25.
- GARRETT, C. J. R. 1970 Bottomless harbours. *J. Fluid Mech.* **43**, 433-449.
- GARRETT, C. J. R. 1971 Wave forces on a circular dock. *J. Fluid Mech.* **46**, 129-139.
- HASKIND, M. D. 1957 The exciting forces and wetting of ships in waves. *Izv. Akad. Nauk S.S.S.R., Otd. Tekh. Nauk* **7**, 65-79. (English trans. *David Taylor, Model Basin Trans.* no. 307.)
- LIGHTHILL, J. 1979 Two-dimensional analyses related to wave-energy extraction by submerged resonant ducts. *J. Fluid Mech.* **91**, 253-317.
- MILES, J. W. & GILBERT, F. 1968 Scattering of gravity waves by a circular dock. *J. Fluid Mech.* **34**, 783-793.
- NEWMAN, J. N. 1962 The exciting forces on fixed bodies in waves. *J. Ship Res.* **6**, 10-17.
- NEWMAN, J. N. 1977 *Marine Hydrodynamics*. Massachusetts Institute of Technology Press.
- OGILVIE, T. F. 1963 First- and second-order forces on a cylinder submerged under a free surface. *J. Fluid Mech.* **16**, 451-472.
- SIMON, M. 1981 Wave-energy extraction by a submerged cylindrical resonant duct. *J. Fluid Mech.* **104**, 159-187.
- SROKOSZ, M. A. 1979 The submerged sphere as an absorber of wave power. *J. Fluid Mech.* **95**, 717-741.